SAND2015-7042C

Observation and Simulation of Motion and Deformation for Impact-Loaded Metal Cylinders

R. J. Hickman[1,a)], J. L. Wise[1,b)], J. A. Smith[1)], J. P. Mersch[1)], C. V. Robino[1)], J. G. Arguello[1)]

[1]Sandia National Laboratories*, P.O. Box 5800, Albuquerque, NM 87185

Corresponding authors: [a)]rjhickm@sandia.gov; [b)]jlwise@sandia.gov

Abstract. Complementary gas-gun experiments and computational simulations have examined the time-resolved motion and post-mortem deformation of cylindrical metal samples subjected to impact loading. The effect of propagation distance on a compressive waveform generated in a sample by planar impact at one end was determined using a velocity interferometer to track the longitudinal motion at the center of the opposing rear (i.e., free) surface. Samples (25.4-mm diameter) were fabricated from aluminum (types 6061 and 7075), copper (OFHC = oxygen free, high conductivity), stainless steel (type 316), and cobalt alloy L-605 (AMS 5759; also referenced as Haynes®25 alloy). For each material, waveforms obtained for a 25.4-mm long cylinder corresponded to two-dimensional strain at the measurement point. The wave-profile data have been analyzed to (i) establish key dynamic material modeling parameters, (ii) assess the functionality of the Sierra Solid Mechanics-Presto (Sierra/SM) code, and (iii) identify the need for additional testing, material modeling, and/or code development. The results of subsequent simulations have been compared to benchmark recovery experiments that showed the residual plastic deformation incurred by cylinders following end, side, and corner impacts.

*Sandia National Laboratories is a multi-program laboratory managed and operated by Sandia Corporation, a wholly owned subsidiary of Lockheed Martin Corporation, for the U.S. Department of Energy's National Nuclear Security Administration under contract DE-AC04-94AL85000.

1. INTRODUCTION

This research effort was motivated by requirements for testing and analysis pertinent to (1) the development and demonstration of an experimental configuration allowing impact loading, time-resolved observation, and subsequent soft recovery of cylindrical metal samples, and (2) the generation of baseline dynamic response data and post-mortem deformation measurements supporting parameter selection and material model validation for multi-dimensional code simulations. Multi-axial strains in different cylinder materials were generated by end-on, side, and corner impacts. The tests (Section 2) were simulated (Section 3) using the transient dynamic module of the multi-dimensional finite element (FE) Sierra Solid Mechanics (Sierra/SM) code[1], which has been developed at Sandia National Laboratories. Material properties for these simulations, including temperature- and rate-dependent effects, were specified on the basis of published constitutive parameters for the respective test materials. Parameter value selections were evaluated on the basis of their utilization with two different material models implemented within Sierra/SM to predict the time-dependent motion of the test cylinders as well as their final deformation. Deformation maps extracted from computational results were compared to the results of post-test 3-D scanner measurements on actual test samples (Section 4), and the simulated time-dependent motion of cylinders that were impacted end-on has been overlaid with velocity interferometer data (Section 5).

2. TESTING

Cylindrical slugs, nominally 25.4-mm thick x 25.4-mm diameter, of different metals were impacted at standardized incidence velocities of 150 and 240 m/s. These shots were conducted at Sandia's Dynamic Integrated Compression Experimental (DICE) Facility using the gas gun illustrated in Figure 1.

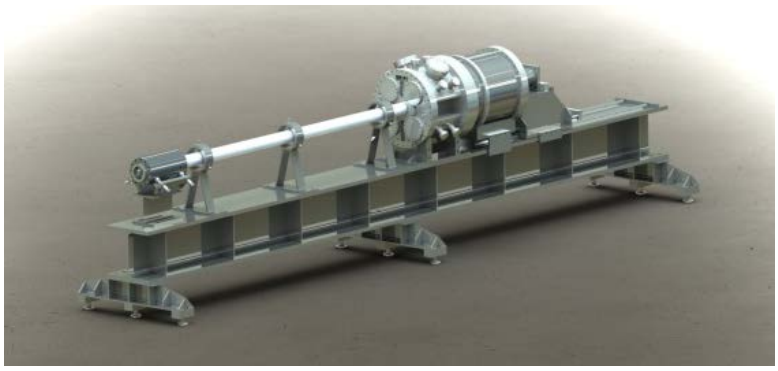

FIGURE 1. Single-stage, 76-mm bore gas gun located at Sandia's DICE Facility.

A slug, or "plug," of test material was mounted in 32 kg/m^3 polyurethane foam that was supported by an aluminum target ring. The slug was positioned in the foam such that the initial impact point, line, or surface was coplanar with the forward face of the target ring. The overall test setup appears in Figure 2. The completed target assembly was installed in the impact chamber approximately 6 mm from the muzzle of the gun, which launched a projectile assembly consisting of a leading 4340 steel impactor/flyer plate (Rockwell C hardness = 52 – 56), a cylindrical projectile body, and a back plate.

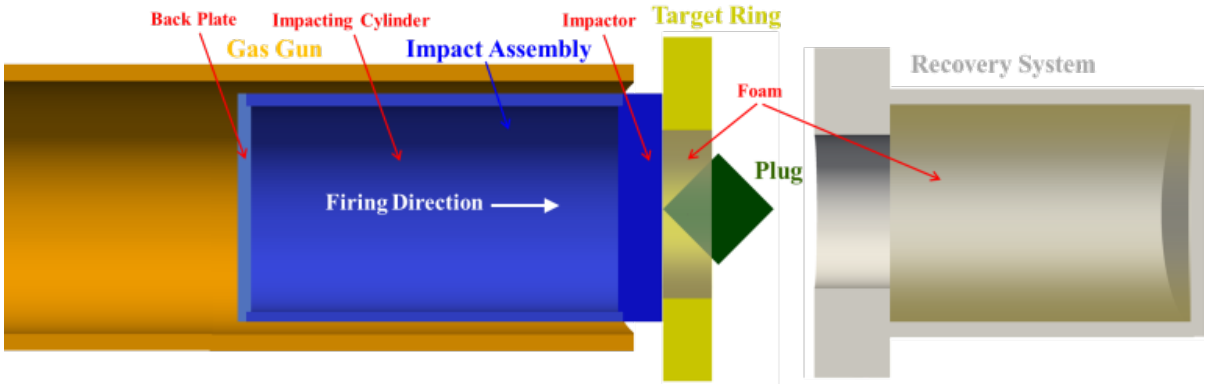

FIGURE 2. Impact test configuration, including gas-gun barrel, projectile assembly with steel impactor/flyer plate, target assembly with test plug/slug, and recovery fixture.

For each experiment, the cylindrical plug was oriented to achieve either a corner (45^0), side, or end-on impact. A dynamic sample recovery system decelerated the test specimen without inducing further damage. This system utilized 128 kg/m^3 polyurethane open-cell foam and stack rubber pads of increasing density to capture the plug inside a heavy stainless steel tank. The entrance opening of the recovery fixture was slightly larger than the sample, but smaller than the impacting flyer plate, thereby allowing passage of the sample but excluding other debris that could produce secondary impacts with the sample. This fixture was positioned 50 – 80 mm downstream of the target ring and was precisely aligned prior to each shot. Following recovery, a 3-D scanning system mapped the slug surface for later comparison with computational results.

3. MODELING

A material constitutive model that includes rate and temperature dependence was desired for this work. Based on a review of published results and the available Sierra/SM options, three constitutive models were considered for the analysis, namely the Material Threshold Stress (MTS)[2,3], Johnson-Cook[4], and Zerilli-Armstrong[5] models. Although the MTS model is included in Sierra/SM, there was uncertainty with respect to assigning the published variables to parameters required to implement the model. Early simulations with this model exhibited deformations that were

significantly different from the results using the Johnson-Cook and Zerilli-Armstrong models. In addition, the Johnson-Cook and Zerilli-Armstrong parameters are more readily available in the literature for the other materials; therefore, it was decided to focus the study on these two models. Cobalt alloy L-605 (AMS 5759; Haynes®25) material parameters for the Johnson-Cook and Zerilli-Armstrong models were provided by Chen[7]. This further motivated a literature search for published parameters associated with the other materials involved in the testing (i.e., 6061 and 7075 aluminum, 316L stainless steel, OFHC copper, and 4340 steel).

Each of the six materials was modeled using the Johnson-Cook method. The cobalt alloy was additionally modeled with the Zerilli-Armstrong approach. The material-specific input parameters for these models, respectively, are listed in Tables 1 and 2 where the information source for each material is referenced[6,7; 10-14]. In addition to the parameters given in Table 1, the hourglass stiffness was modified from the default value of 0.05 to minimize element locking observed in preliminary cobalt alloy L-605 (AMS 5759; Haynes®25) simulations; instead, the cobalt alloy slug simulations utilized an hourglass stiffness of 0.001.

Table 1: Johnson-Cook model inputs

Parameter		Units	6061 Al[10]	7075 Al[11]	Haynes®25[6,7]	OFHC Cu[12]	316L SS[13]	4340 Steel[14]
Density	ρ	g/cm^3	2.70	2.81	9.13	8.93	8.00	7.62
Elastic Modulus	E	MPa	$6.89\cdot10^4$	$7.17\cdot10^4$	$2.10\cdot10^5$	$1.25\cdot10^5$	$2.10\cdot10^5$	$2.10\cdot10^5$
Poisson's Ratio	ν	–	0.33	0.33	0.296	0.34	0.29	0.30
Yield Stress	σ_y	MPa	289.6	517	455	90	304.98	1716.52
Hardening Constant	B	MPa	203.4	405	2475	292	441.01	1087.4
Hardening Exponent	n	–	0.35	0.41	0.9	0.31	0.1	0.26
Density*Specific Heat	ρC_v	N/(mm^2·K)	2.4192	2.6976	4.06	3.513	4	3.681
Rate Constant	C	–	0.011	0.0075	0.0235	0.013	0.057	0.014
Thermal Exponent	m	–	1.34	1.1	0.725	1.09	1.041	1.03
Reference Temperature	T_{ref}	K	294.26	293	293	298	273	293
Melt Temperature	T_{melt}	K	925.37	750	1728	1356	2525	1793
edot_ref	$\dot{\varepsilon}_0$	–	–	–	–	–	–	–
Reference Rate	e_{ref}	–	1	0.00016	–	–	–	–

Table 2: Zerilli-Armstrong model inputs

Parameter		Units	Haynes®25[6,7]
Density	ρ	g/cm^3	9.13
Elastic Modulus	E	MPa	$2.10\cdot10^5$
Poisson's Ratio	ν	–	0.296
Yield Stress	σ_y	MPa	100
Initial Density	ρ_{init}	g/cm^3	9.13
ART VIS CL	–	–	0.05
ART VIS CQ	–	–	0.05
Absolute Zero Temperature	T_{abs}	K	0
Initial Temperature	T_{init}	K	298
Specific Heat	C_v	mJ/(g·K)	445
Yield Stress C0	C0	MPa	100
Strain Rate Coefficient C1	C1	MPa	925
Thermal Softening Coefficient C3	C3	K^{-1}	0.0025
Strain Rate Coefficient C4	C4	K^{-1}	0.0001
Strain Hardening Coefficient C5	C5	MPa	2475
Strain Hardening Exponent	n	–	1.075
Grüneisen parameter	g	–	0
Mie-Grüneisen K2 parameter	K2	MPa	0
Mie-Grüneisen K3 parameter	K3	MPa	0
Maximum Tensile Pressure	p_{max}	MPa	8000

4. COMPARISON OF SIMULATION AND TEST DEFORMATION RESULTS

For each test and analogous simulation, representative linear dimensions were determined and a figure was constructed to present test and simulation geometries side-by-side. While individual dimensional measurements provided a means for quantifying differences in test and simulation results, the post-test specimen scans afforded an

opportunity to visually assess local and global deformations *vis-à-vis* the computations. For example, features such as "lips" on the edges of impacted surfaces and the curved outlines of these flattened faces are much easier to examine and compare using the scans. A representative set of simulation and test results for the deformation of impact-loaded 7075 aluminum cylinders is shown in Figure 3.

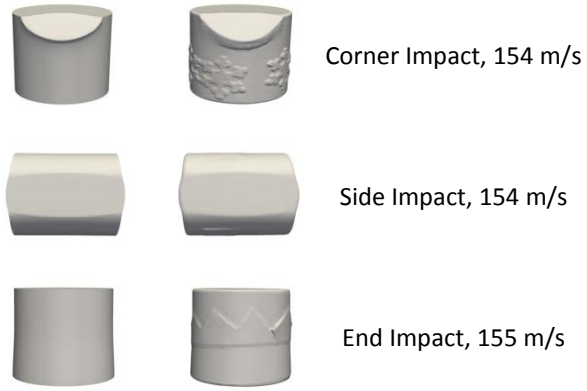

FIGURE 3. Simulated (left) and actual (right) deformation of 7075 aluminum tests slugs subjected, respectively, to corner, side, and end impacts.

5. VISAR MEASUREMENTS

A velocity interferometer system (VISAR[15]) was employed during several shots involving samples experiencing an end-on impact to acquire time-resolved measurements that complemented the post-test 3-D scan data. A waveform (i.e., velocity history) corresponding to longitudinal free-surface motion under multi-axial strain conditions was obtained for a 25.4-mm thick x 25.4-mm long sample of each material. Figure 4 illustrates the typical VISAR experimental setup. The same nominal impact velocity of 150 m/s was used for each of the VISAR shots.

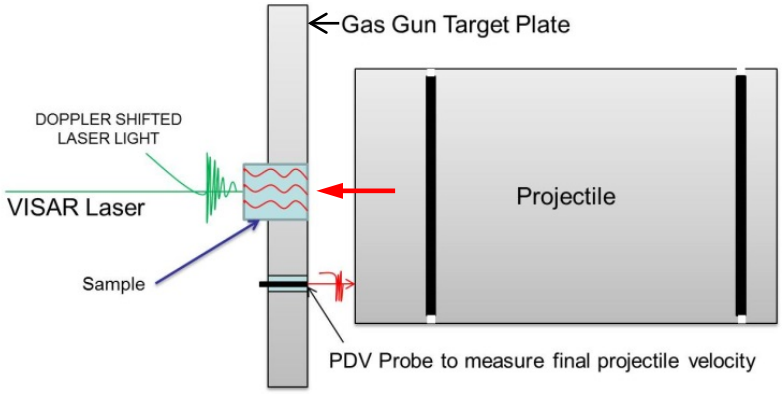

FIGURE 4. Typical VISAR experiment configuration.

As shown in Figure 5, the velocity interferometer data were compared on a sample-by-sample basis to corresponding Sierra/SM numerical simulations for the sake of assessing the functionality of the code and material models. Based on these overlays, the dynamic material modeling and associated numerical simulations yield results that compare very acceptably with the acquired waveforms for all five cylinder compositions.

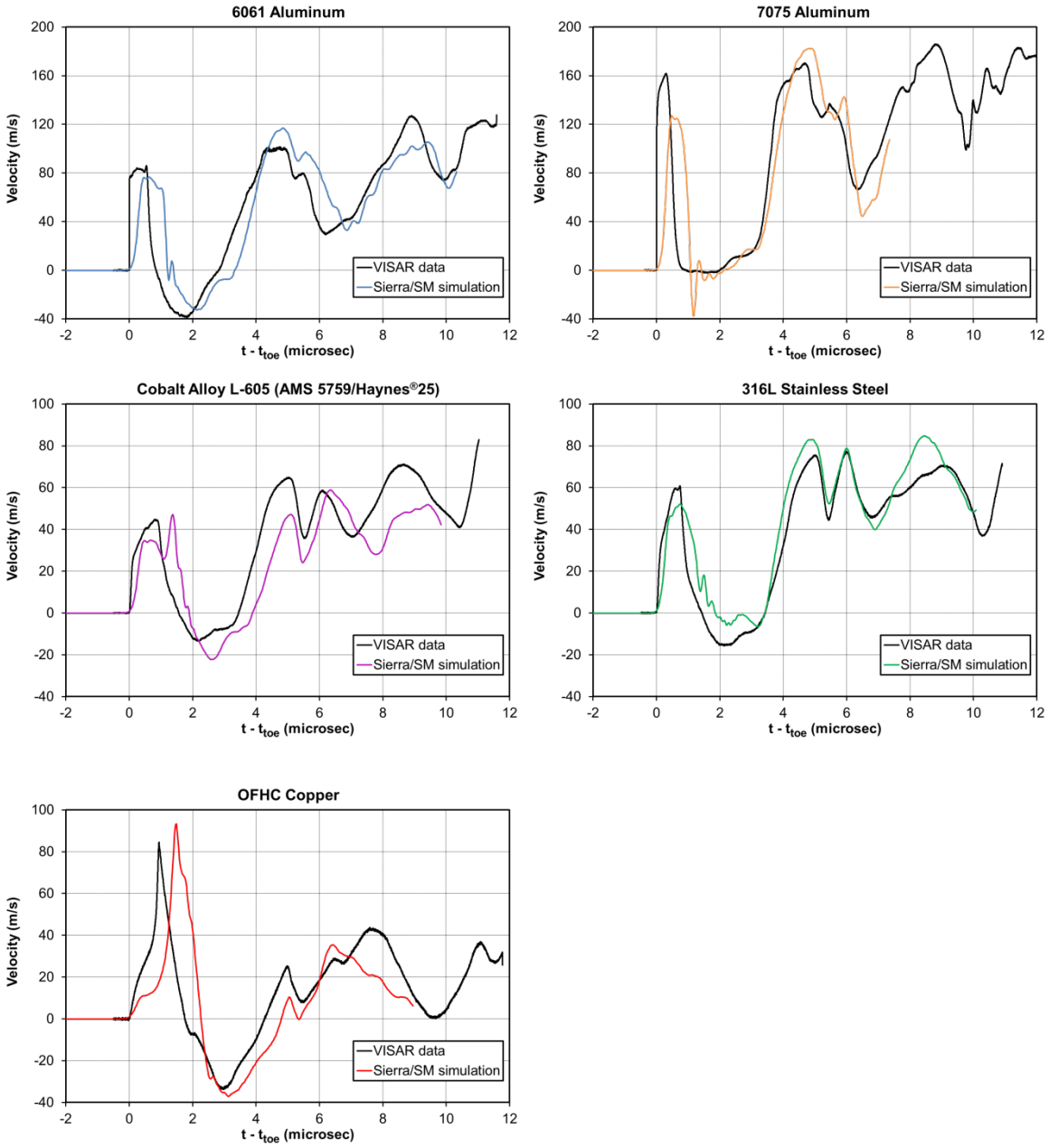

FIGURE 5. Comparison of Sierra/SM simulations with respective VISAR measurements for cylinders fabricated from 6061 aluminum, 7075 aluminum, L-605 cobalt alloy, 316L stainless steel, and OFHC copper.

6. SUMMARY

Sierra/SM simulations employing the selected dynamic material models replicated post-test measurements of global deformations within 11 percent for impacts at both 150 and 240 m/s; in fact, the agreement between predicted and measured deformations was typically within 5 percent. Some localized deformation was not reproduced by the analysis, but it was minor in scale with respect to the global deformation of the specimen. The combination of time-resolved interferometer data and post-shot deformation measurements provides an excellent methodology for assessing code performance and the validity of material models. Comprehensive coverage of the recovery testing and 3-D modeling results is detailed in a recent Sandia report[16].

REFERENCES

1. SIERRA Solid Mechanics Team, Sierra/SolidMechanics 4.34 User's Guide, Sandia National Laboratories, Albuquerque, NM (2014).
2. P. S. Follansbee and U. F. Kocks, Acta metal**. 36d**, No. 1, 81 – 93 (1988).
3. P. S. Follansbee and G. T.Gray III, Metall. Trans. A **20A**, 863 – 874 (1989).
4. G. R. Johnson and W. H. Cook, Proc. 7th Int. Symp. on Ballistics, The Hague, The Netherlands, 541 – 547 (1983).
5. F. J. Zerilli and R. W. Armstrong, J. Appl. Phys. **61**, 1816 – 1825 (1987).
6. G. T. Gray III, S. R. Chen, S. R. Bingert, et al., "Unconventionally Processed High-Density Materials," Progress Report FY93, Joint DoD/DOE Munitions Technology Program, 33 – 68 (1993).
7. S. R. Chen, "Constitutive Modeling of Haynes Alloys," personal communication, Los Alamos National Laboratories, Los Alamos, NM (2014).
8. SIERRA Solid Mechanics Team, Sierra/SolidMechanics 4.34 User's Guide: Addendum for Shock Capabilities, Sandia National Laboratories, Albuquerque, NM (2014).
9. "Viscoplasticity." *Wikipedia*. Wikimedia Foundation, 09 January 2015. Web. 09 February 2015 (http://en.wikipedia.org/wiki/Viscoplasticity).
10. J. Fish, C. Oskay, R. Fan, and R. Barsoum, "Al 6061-T6 – elastomer impact simulations," Electronic document, https://www.scorec.rpi.edu/REPORTS/2005-11.pdf (2005).
11. E. Corona and G. E. Orient, "An Evaluation of the Johnson-Cook Model to Simulate Puncture of 7075 Aluminum Plates," SAND2014-1550, Sandia National Laboratories, Albuquerque, NM (2014).
12. T. J. Holmquist and G. R. Johnson, Journal De Physique IV, Colleque C3, suppl. Au Journal de Physique III, Vol. **1** (1991).
13. H. Chandrasekaran and R. M'Saoubi, Machine Science and Technology **9**, 131 – 145 (2005).
14. B. Banerjee, Int. J. Solids and Structures **44**, 834 – 859 (2007).
15. L. M. Barker and R. E. Hollenbach, J. Appl. Phys. **43**, 4669 – 4675 (1972).
16. J. A. Smith, J. P. Mersch, R. J. Hickman, and J. L. Wise, "Impact Testing and Analysis of Metal Slugs," SAND2015-4578, Sandia National Laboratories, Albuquerque, NM (2015).